Could Kīlauea's 2020 post caldera-forming eruption have been anticipated?

Paul Segall[1], Kyle Anderson[2], Taiyi A. Wang[1]

[1]Department of Geophysics, Stanford University

[2]U. S. Geological Survey, Volcano Science Center

Key Points:

- Time predictable estimate from 2018 erupted volume and long term magma supply rate greatly overestimates the post 2018 repose period.
- Modeling magma surges following collapse events shows driving pressures at the end of collapse cycles was only ~ 1 MPa.
- We estimate a 73% chance of pressure sufficient to raise magma to the 12/20/2020 eruptive vents based on GPS data up to that date.

Abstract

In 2018 Kīlauea volcano erupted a decade's worth of basalt, given estimated magma supply rates, triggering caldera collapse. Yet, less than 2.5 years later Kīlauea erupted again. At the 2018 eruption onset, the pressure within the shallow summit reservoir was ~ 20 MPa above magmastatic as implied by the elevation of the primary vent. By the onset of collapse this decreased by ~ 17 MPa (Anderson et al., 2019). Analysis of magma surges observed following collapse events implies that excess pressure at the eruption end was only ~ 1 MPa. Given the elevation difference between the 2018 and 2020 vents, we estimate ~ 11.5 MPa pressure increase was required to bring magma to the surface in December 2020. Analysis of GPS data between 8/2018 and 12/2020 shows there were even odds this condition was met 9 months before the 2020 eruption, and 73% probability on the day of the eruption.

Corresponding author: Paul Segall, `segall@stanford.edu`

Plain Language Summary

In 2018 Kīlauea volcano erupted so much lava that, based on long-term magma supply rates, one might have anticipated a long quiescent period. Yet Kīlauea erupted again in 2020, less than 2.5 years later. Deformations of the surface can be used to infer pressure changes within the magma system, but significant inelastic deformations during the 2018 caldera collapse make this approach challenging. In this study, we bring diverse observations together to infer the history of pressure changes within the magma system during the inter-eruptive period. Analysis of surges in eruptive rates following caldera collapse events suggests that driving pressure – pressure in excess of magmastatic – was only ~ 1 MPa at the end of the 2018 eruption. Based on the elevation difference between the 2018 and 2020 eruptive fissures, we estimate the pressure increase necessary to bring magma to the 2020 vents. Analysis of GPS data between 8/2018 and 12/2020 shows there was a 73% probability that this condition was met at the onset of the 2020 eruption, and even odds 9 months before the eruption.

1 Introduction

Between May 1 and August 4, 2018 Kīlauea erupted between 0.9 and 1.4 cubic kilometers of basalt DRE (Dietterich et al., 2021), causing collapse of the pre-existing summit caldera. Dzurisin & Poland (2018) summarize numerous estimates of average magma supply rate to Kīlauea, with most longer term estimates in the range of 0.1 $\pm$0.02 km^3/yr. Given a supply rate of 0.1 km^3/yr, one might have anticipated a decade long pause in eruptive activity. Indeed, only a few small eruptions occurred in the decade following the 1924 summit collapse, with a complete absence in the subsequent 18 years (Wright & Klein, 2014; Neal et al., 2019). At the same time, Neal et al. (2019) noted that the large pressure drop in 2018 increased the pressure gradient driving recharge into Kīlauea's summit magma system, and concluded "The next several years offer an exceptional and exciting opportunity to study the evolution of magmatism following a major perturbation to Kīlauea's plumbing system."

In fact, a summit eruption began on December 20, 2020, less than two and a half years after the 2018 eruption ceased. Clearly, a constant recharge rate and threshold magma volume was not a good predictor of future eruptive activity.

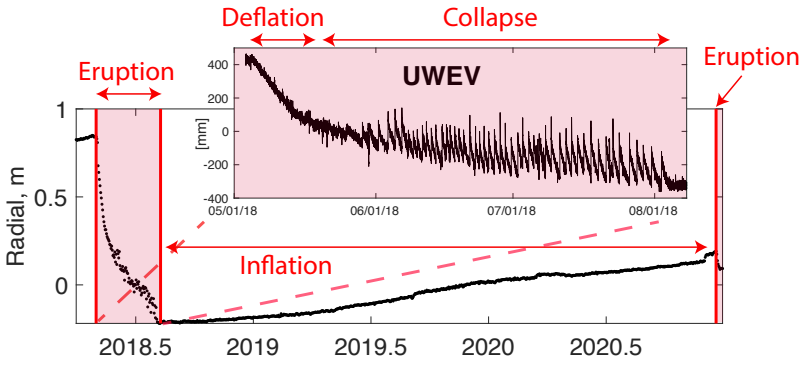

Figure 1. Radial component of displacement at GPS station UWEV. Daily solutions are shown for the entire time period, with higher rate data during the 2018 eruption to illustrate episodic inflation-deflation cycles during discrete collapse events.

Magma chamber pressure should be a better indicator of eruptability. Pressure sufficient to raise a column of magma from the shallow reservoir to the surface is a necessary, but not necessarily sufficient, condition for an eruption. In an elastic system surface deformations are proportional to changes in magma pressure. In some cases eruptions have occurred when inflation restored the previous co-eruptive deflation, for example at Krafla, Iceland in the 1970s (Sturkell et al., 2006), or at Axial Seamount (Nooner & Chadwick, 2016). Whether or not volcanoes are "inflation predictable" depends on a number of factors, including whether significant inelastic deformation occurs (Segall, 2013). The massive collapse of Kīlauea in 2018 was dominated by inelastic deformation, which precludes conventional elastic modeling during this period. Nevertheless, we show that careful accounting of changes in summit reservoir pressure between the beginning of the 2018 eruption and the onset of the 2020 eruption could have flagged the potential for renewed activity.

Figure 1 shows the radial displacements of GPS station UWEV on the north rim of Kīlauea caldera. This figure makes clear that the inter-eruption inflation between August 2018 and December 2020 was much smaller than the co-eruptive inward directed displacement in 2018 – we refrain from labeling it deflation as it involved inelastic deformation. However, during the first two weeks of the eruption in May 2018, prior to the onset of episodic collapse, the summit apparently deflated elastically. Anderson et al. (2019) combined measurements of magma draining from the Overlook vent (until it disappeared on May 10) with tilt and GPS data to infer that pressure in the shallow Halema‘uma‘u

reservoir declined by $\sim 17.2 \pm 1.1$ MPa at the onset of the first collapse event on 16 May 2018.

At the onset of the 2018 eruption the magma level in the Overlook vent was 800 meters above the principal Fissure 8 vent in the Lower East Rift Zone (LERZ). For plausible estimates of magma density, this corresponds to a net pressure difference of 20 MPa (we estimate $\pm$ 1 MPa to account for uncertainty in density (Anderson et al., 2019)). Given the estimated elastic pressure drop of 17.2 ± 1.1 MPa, this leaves a driving pressure (pressure over magmastatic from the Halema‘uma‘u reservoir to Fissure 8) of 2.8 $\pm$ 1.1 MPa at the onset of caldera collapse (Table 1).

During the 2018 eruption, deformation time series, both GPS (Figure 1) and tilt, exhibit continued radially inward and downward motion (Anderson & Johanson, in review; Tepp et al., 2020), perhaps suggesting a further decrease in pressure. However, the inelastic deformation necessitates new approaches for determining magma chamber pressure during this period. Here we make use of magma surges at Fissure 8 following collapse events, described by Patrick et al. (2019), to estimate the driving pressure in the summit magma system during this phase of the eruption. Beginning in July, Patrick et al. (2019) noted surges in the effusion rate from ~ 150 m^3/s DRE immediately prior to collapse events, to $400-500$ m^3/s following collapses, a factor of three increase. From analysis of co-collapse deformation at Kīlauea's summit, Segall et al. (2020) estimated that individual collapse events caused pressure increases within the shallow Halema‘uma‘u reservoir of ~ 3 MPa. Wang et al. (2022) estimate the pressure increment to be 1.9 MPa, from a combination of seismic and geodetic data. For pressure changes of $2 - 3$ MPa to cause a factor of three change in volume flux implies that the average driving pressure must have been quite low. We quantify this further in the following section.

2 Implications of Magma Surges for Summit Reservoir Pressure

Peak LERZ effusion rates were delayed by two to four hours (possibly up to 5 hours) following collapse events, suggesting the influence of magma storage zones between the Halema‘uma‘u reservoir and Fissure 8. Previous studies have identified geodetic and petrologic evidence for magma storage zones within the ERZ (Owen et al., 2000; Thornber et al., 2003). In addition, some of the early erupted lavas in 2018 were chemically evolved indicating prolonged storage within the ERZ (Gansecki et al., 2019), as had been noted

for previous ERZ eruptions. For simplicity, we model these storage zones as fluid-filled reservoirs within an elastic crust.

For laminar flow in conduits that don't dilate significantly with pressure perturbations, the mass flux q is proportional to the pressure difference in excess of magmastatic; $q = k(\Delta p - \rho g h)$, where k depends on conduit shape, aperture, and magma viscosity, and h is elevation difference. Combining this with mass conservation and a linearized equation of state in terms of magma compressibility β_m, leads to a first order system of equations in pressure p, which for two reservoirs (Figure 2A) with pressures p_1, p_2 is

$$\frac{dp_1}{dt} = \frac{-k_1(p_1 - \rho g h_{12} - p_2)}{V_1 \beta_1} \tag{1a}$$

$$\frac{dp_2}{dt} = \frac{k_1(p_1 - \rho g h_{12} - p_2)}{V_2 \beta_2} - \frac{k_2(p_2 - \rho g h_{2v})}{V_2 \beta_2} \tag{1b}$$

where $\beta_i, (i = 1, 2)$ is the net compressibility, the sum of the magma and chamber compressibility, $\beta_c \equiv (1/V)dV/dp$; h_{12} is the elevation difference between reservoirs 1 and 2, and h_{2v} is the elevation difference between reservoir 2 and the LERZ vent. Equations (1) can be written compactly as

$$\frac{d\mathbf{p}}{dt} = A\mathbf{p} + \mathbf{B}, \tag{2}$$

where $\mathbf{p} = [p_1, p_2]^T$. The solution to the homogeneous equations, $d\mathbf{p}/dt = A\mathbf{p}$ depend on the eigenvalues, λ and eigenvectors Ψ of A,

$$\mathbf{p}(t) = c_1 \Psi_1 e^{\lambda_1 t} + c_2 \Psi_2 e^{\lambda_2 t} \equiv \Phi(t)\mathbf{c}, \tag{3}$$

where $\mathbf{c}$ are constants determined by initial conditions, and $\Phi(t)$ is known as the *fundamental matrix*. The particular solution $\mathbf{p}_p$ is found by noting that $\mathbf{B}$ is time invariant, so that $\mathbf{p}_p = -A^{-1}\mathbf{B}$, and the general solution is

$$\mathbf{p}(t) = \Phi(t)\mathbf{c} - A^{-1}\mathbf{B}. \tag{4}$$

Note that this approach can be easily extended to N magma reservoirs, with the general solution being the sum of N exponentials.

The coefficients **c** are determined by initial conditions at the onsets of collapse cycles. For the erupted flux to be continuous, the ERZ reservoir pressure at the end of a cycle (with duration T =1.4 days, on average in 2018) must equal the pressure at the beginning of the cycle, $p_2(t=0) = p_2(t=T)$. For the summit reservoir $p_1(t=0) = p_1(t=T) + \Delta P$, where ΔP is the pressure change induced by collapse. (Segall et al. (2020) found that, constraining the ring fault to be vertical, $\Delta p = 3 \pm 0.3$ MPa.) In matrix form,

$$\mathbf{p}(t=0) = \mathbf{p}(t=T) + \begin{bmatrix} \Delta P \\ 0 \end{bmatrix}, \tag{5}$$

which when combined with (4) leads to

$$\mathbf{p}(t) = \Phi(t)\left[\Phi(0) - \Phi(T)\right]^{-1} \begin{bmatrix} \Delta P \\ 0 \end{bmatrix} - A^{-1}\mathbf{B}. \tag{6}$$

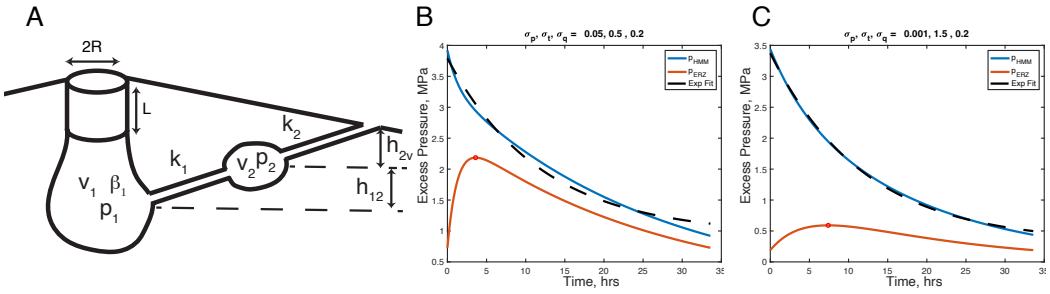

Figure 2. A) Definition sketch of magmatic system with summit reservoir below caldera block, and a single ERZ reservoir. V_i and β_i refer to reservoir volume and total compressibility, respectively. k_i are the transmissivities, and h_i are elevation differences. B,C) Estimated reservoir pressures from fit to surge data. p_{HMM} is summit pressure, dashed line exponential fit, p_{ERZ} is East Rift Zone reservoir pressure. Circle is maximum pressure in the ERZ reservoir. B) Nominal weights, C) Weights adjusted to improve exponential fit to summit pressure history.

From the data in Patrick et al. (2019) we take the ratio of fluxes $max(q)/min(q) = max(p_2)/min(p_2)$ to be a factor of three. The time of peak flux, and thus time at which p_2 peaks, is taken to be $t = 2{-}3$ hours, although as noted it could be somewhat longer. The third constraint comes from intra-collapse deformation at Kīlauea summit (at GPS/tilt stations other than UWEV/UWD) which shows a nearly exponential decay with a time

constant of $\sim$ 12 hours (Segall & Anderson, 2021). We thus minimize the difference between the best fitting exponential curve with decay time of 12 hours (a proxy for the inter-collapse deformation data) and the predicted $p_1(t)$, measured at N discrete times. The estimated parameters consist of the transmissivities, $k_i, (i = 1, 2)$, the product V_i, β_i, and the elevation differences h_{12} and h_{2v}. We adopt a quadratic objective function, consistent with normally distributed errors,

$$\frac{1}{N}\sum_{k=1}^{N}\frac{(p_1(t_k)-\hat{p}_1(t_k))^2}{\sigma_p^2}+\frac{(t(max(p_2))-2.5)^2}{\sigma_t^2}+\frac{(max(p_2)/min(p_2)-3)^2}{\sigma_q^2} \tag{7}$$

where $\hat{p}_1$ indicates predicted pressure, and σ_p, σ_t and σ_q adjust the weights on the different components of the objective. The duration of the collapse cycle is $T = 1.4$ days, and the pressure increment at $t = 0$ is $\Delta p = 3$ MPa.

For nominal weights of $\sigma_p = 0.05$ MPa, $\sigma_t = 0.5$ hrs, and $\sigma_q = 0.2$, the best fitting solution has a max/min pressure ratio of 3.0 in the ERZ reservoir, and the time of peak pressure is 3.6 hours post collapse. The fit to the exponential decay is not ideal, however (Figure 2B). Increasing the weight on the exponential decay ($\sigma_p = 0.001$ MPa) at the expense of the time of peak flux, ($\sigma_t = 1.5$ hrs) improves the fit to the exponential decay, but causes the peak pressure to be delayed to 7.4 hours post collapse. In this case the max/min pressure ratio is 3.1 (Figure 2C). While neither model fits all of the data perfectly, indicating limitations in the forward model, in both cases the summit reservoir pressure at the end of the cycle is quite low: 0.9 MPa in the nominal model and 0.4 MPa in the second case. Similar results have been obtained with models containing three reservoirs. Anderson & Johanson (in review) similarly conclude that the driving pressure was low, on the order of 1.3 to 1.9 MPa at the end of a collapse cycle, although they did not fit the time dependence. Since the eruption ended late in the ultimate collapse cycle, we conclude that *the driving pressure at the end of the eruption was on the order of only 1 MPa.*

3 Summit Reservoir Pressure History

Analysis of LERZ magma surges suggests that the driving pressure at the end of the 2018 eruption was on the order of 1 MPa. The December 2020 fissures and lava lake were $\sim$ 300 m below the elevation of the 2018 Overlook vent, and 500 m above Fissure 8. This is equivalent to a driving pressure of 12 to 13 MPa, relative to a Fissure 8 da-

tum. Given a post-2018 pressure of ~ 1 MPa, this suggests that a pressure increase of 11.5 ± 1 MPa was necessary to bring magma to the elevation of the 2020 vents (Table 1). We next explore whether deformation measurements during the inter-eruptive period could have revealed such a pressure increase.

Table 1. Pressure history. Pressures in excess of magmastatic relative to Fissure 8 datum.

Description	Pressure (MPa)
2018 Initial Pressure	20 ± 1
Deflation at onset of collapse	-17.2 ± 1.1
Driving pressure at onset of collapse	2.8 ± 1.4
Pressure required for 2020 onset	12.5 ± 1
Less driving pressure at 2018 eruption end	- ~ 1
Pressure increase required for 2020 onset	11.5 ± 1

We analyze data from August 2018 to December 2020 to estimate the pressure change within the shallow Halemaʻumaʻu (HMM) reservoir. Previously, Wang et al. (2021) used GPS and InSAR time series to investigate the post-2018 eruptive period, up to December 2019. These data show that early in the post-eruptive period, HMM inflated while the deeper South Caldera (SC) reservoir deflated. They estimated the geometry of these reservoirs (assumed ellipsoidal) with the HMM volume constrained to the median value estimated by Anderson et al. (2019) based on pre-eruptive deflation and draining of the Overlook vent (3.9 km^3). Due to the inherent trade-off in reservoir volume and pressure change, Wang et al. (2021) were not able to constrain the volume of the SC reservoir.

We extend the Wang et al. (2021) analysis to include GPS data for the full time period between the two eruptions, employing all continuous GPS stations in the Kīlauea summit region, with the exception of CALS which is located on the down-dropped block. We remove minor displacements associated with a small dike intrusion in the summit area on December 2, 2020 (we do not account for potential influence on reservoir pressure change, which is likely minor). The results indicate that the pressure increase exceeded the 11.5 ± 1 MPa threshold by some point in 2020 (Figure 3a).

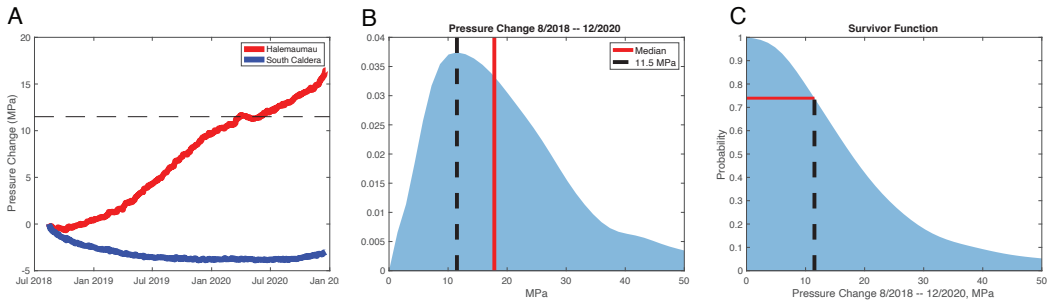

Figure 3. Inter-eruptive pressure change estimate from GPS data. A) Pressure history in the two summit reservoirs assuming the MAP reservoir geometry of Wang et al. (2021). B) PDF of net pressure change between 8/2018 and 12/2020 accounting for uncertainty in the HMM reservoir volume from Anderson et al. (2019) and other reservoir parameters from Wang et al. (2021). C) The survivor function corresponding to the PDF in B.

This result is incomplete however, because it does not account for uncertainty in the HMM chamber volume, which directly trades off with the inferred pressure change. To account for this, we resampled from the posterior distribution of chamber geometry (e.g., aspect ratio, location) from Wang et al. (2021) as well as HMM volume from Anderson et al. (2019). To account for volume decrease due to caldera collapse we subtract the 2018 caldera volume (0.8 km^3) from the HMM volume, but limit the results to be greater than the smallest volume in the pre-collapse posterior distribution (0.45 km^3). The resulting probability distribution for net pressure increase up to the December 20, 2022 eruption (Figure 3b) is thus skewed to high values (small chamber volumes). The median value significantly exceeds the estimated threshold. Indeed, the survivor distribution (one minus the cumulative distribution function) indicates a 73% probability that the pressure increase exceeded the 11.5 MPa threshold. Thus, it should have been possible to conclude in December 2020 that there was reasonable probability of sufficient pressure within the HMM reservoir to erupt magma within the deep pit left by the 2018 collapse. The December 2, 2020 dike intrusion further supports a relatively high summit magma pressure.

The median model fits the cumulative GPS displacements reasonably well (Figure 4). Under prediction of horizontal displacements at the more southerly stations, DEVL, AHUP, and PUHI may be due, at least in part, to neglect of south flank motion.

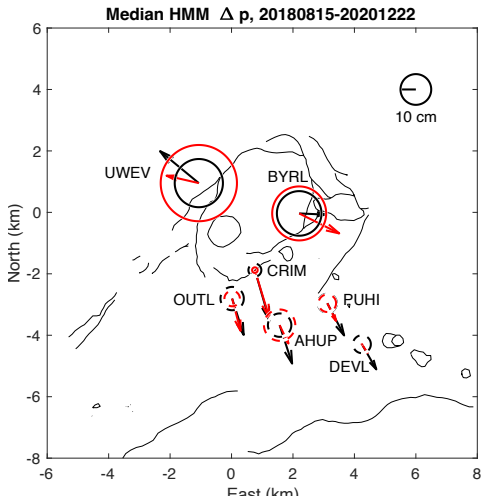

Figure 4. Observed (black) and predicted (red) displacements during the interval 08/15/2018 – 12/22/2020 for the model corresponding to the median pressure change. Circles indicate vertical displacements, dashed for subsidence.

4 Discussion

As noted above, pressure sufficient to bring magma to the surface is a necessary but insufficient condition for an eruption. The other requirement is a pre-existing conduit or sufficient pressure to propagate a dike to the surface. To assess the latter requires knowledge of the *in situ* stress state, which could be quite spatially variable in the vicinity of the HMM reservoir. If the stress is somewhat extensional, as seems likely given south flank spreading, it could be that magmastatic pressure is sufficient to dilate a dike. The results in Figure 3B could indicate that a pressure several MPa greater than magmastatic was required to initiate the 2020 eruption, but given uncertainties we do not believe the difference is significant. We further note that the uncertainty in estimating the pressure change from the GPS data far exceeds the uncertainty in the value of the threshold pressure.

4.1 Time to Possible Eruption

We use the results of Section 3 to determine how the probability of eruption increased with time through 2020. The distribution of cumulative pressure changes (Figure 3b) is used to scale the HMM pressure history for the MAP model of Wang et al. (2021) (Figure 3a), yielding a distribution of pressure histories consistent with the range of accept-

able chamber geometries. From this we determine the distribution of times, t_{thresh}, at which the HMM pressure reached the threshold of 11.5 MPa. Of course, for some reservoir models the threshold is not met by the time of the eruption; the cumulative distribution of t_{thresh} is 0.73 on that day (Figure 3c). We find that probability $p = p_{thresh}$ reached 0.5 on 3/11/2020, 0.6 on 8/4/2020, and 0.7 on 11/26/2020. That is, by the end of February there were even odds that the pressure in the HMM reservoir was sufficient to raise magma to the surface. By the time of the December 2 dike intrusion, that probability had increased to 70%. The CDF is shown in Supplementary Information.

4.2 Non-deformable Conduits

The surge model assumes non-deforming conduits. When a conduit is sufficiently narrow (dike-like) that pressure-induced displacements are significant, conduit pressure follows a nonlinear diffusion equation (Montagna & Gonnermann, 2013). Specifically, they show that non linear effects are significant when the ratio of displacement to dike aperture ϵ, exceed roughly 0.25.

Gonnermann et al. (2019) considered such a model to explain the time history of tilts along the ERZ as well as effusion surges. For the 2018 eruption, the dike would also need to have sufficiently high transmissivity to explain the average volume flux of ~ 300 m^3/s (the average of the Patrick et al. (2019) values). The volume flux q is proportional to pressure gradient, dP/dx, dike height h, and the cube of the aperture. Solving for the required dike height (see Supplementary Information), yields

$$h = \left[\frac{12\eta q}{\alpha^3 (dP/dx)}\right]^{1/4} \qquad \alpha \equiv \frac{2(1-\nu)\Delta P}{\mu\epsilon}, \tag{8}$$

where η is viscosity (100 Pa-s), and dP/dx the down-rift pressure gradient in excess of magmastatic. We estimate the latter as 2.8 MPa (the excess pressure at the start of collapse) over the 40 km distance between the summit and Fissure 8, or 70 Pa/m. μ, ν are shear modulus and Poisson's ratio. For a shear modulus of 3 GPa this yields a dike height of nearly 400 meters. Any conduit shorter than this, capable of transmitting the observed flux, would have a large enough aperture that elastic displacements would be negligible.

For a given volume flux, crack-like conduits lose heat more efficiently than more equi-dimensional conduits. This is why curtain of fire, fissure eruptions rapidly evolve

to isolated vents (Delaney & Pollard, 1981). It is reasonable then to ask whether a 400 meter tall by 2 m wide conduit would persist several months into an eruption. At the surface the 2018 eruption had localized to a single vent (Fissure 8) by May 28 (Neal et al., 2019). The conduit geometry could be variable along strike; the conduit from the summit to Pu'u O'o has existed for decades and is least likely to be crack-like. The conduit could be more cylindrical from the summit to Pu'u O'o and crack-like from there to Fissure 8. It is also possible that magma was transported deeper in the rift system where heat loss would have been less significant. On the other hand, intermediate storage zones are well established in the ERZ. Future modeling should examine the effect of both deformable conduits and ERZ storage zones.

4.3 Implications for Ring Fault Shear Strength

At static equilibrium the weight of the caldera block of radius R is balanced by pressure p at its base and shear stress, τ, on its sides: $\pi R^2 L\rho_c g - \pi R^2 p - 2\pi RL\tau = 0$, where L and ρ_c are block thickness and density. The excess pressure (over magmastatic) acting on the base of the block is $p_{ex} = p - \rho g(L - \Delta h)$, where $\Delta h \simeq 800$ m is the elevation difference between the top of the block and the eruptive vent. Ignoring the slight difference between magma and block density, then $p_{ex} = \rho g \Delta h - 2L\tau/R$, with $\rho g \Delta h \sim$ 20 MPa. The shear stress reaches the frictional strength when the excess pressure is a *minimum*, immediately prior to a collapse. Thus, $\tau_c \simeq (R/2L)(\rho g \Delta h - min(p_{ex}))$. For $R/L \sim 1$ (Anderson et al., 2019), and $min(p_{ex}) \sim 1$ MPa, the frictional strength is of order 9.5 MPa, comparable to estimates of Segall & Anderson (2021) based on dynamical modeling of collapse events.

4.4 Pressure History Post December 2020

The December 2020 eruption lasted until May 2021, and was initially accompanied by a short period of deflation. This was followed by a period of apparent inflation. Inflation during an eruption suggests an increase in viscous pressure loss, potentially due to narrowing of the conduit. The short pause in 2021 ended with a fissure eruption in the bottom of Halema'uma'u crater on September 29, 2021. Inflation in 2021 more than recovered the December 2020 deflation, suggesting the behavior was not "inflation predictable", although the interpretation is complicated by an intrusion in the south caldera region in August of 2021.

5 Conclusion

- A "time predictable" estimate, based on the erupted volume in 2018 and average long term magma supply rate, greatly overestimates the duration of the post 2018 repose period.
- The driving pressure (pressure over magmastatic relative to the primary LERZ vent) in the shallow Halema'uma'u reservoir at the onset of caldera collapse was ~ 3 MPa.
- Modeling variations in magma effusion rates following collapse events suggests driving pressures at the end of collapse cycles, and hence the end of the eruption, of only ~ 1 MPa.
- The elevation difference between the pre-existing lava lake and the December 2020 eruptive vents and lava lake suggests a pressure increase of 11 - 12 MPa to bring magma to the surface in December 2020.
- Analysis of post 2018 continuous GPS data, conditioned on constraints from pre-collapse deflation measurements, demonstrates a 73% probability that there was sufficient pressure to raise magma to the surface condition on December 20, 2020, and that there were even odds as early as 9 months prior to the eruption.

6 Open Research

Software and GPS data is currently available at https://github.com/taiyi-wang/pressure_budget_kilauea and will be linked to Zenodo before final submission.

Acknowledgments

Thanks to Roger Denlinger for comments. Support from National Science Foundation EAR-2040425.

References

Anderson, K. R., & Johanson, I. (in review). Incremental caldera collapse at Kīlauea volcano recorded in ground tilt and high-rate gnss data, with implications for collapse dynamics and the magmatic system.

Anderson, K. R., Johanson, I. A., Patrick, M. R., Gu, M., Segall, P., Poland, M. P., ... Miklius, A. (2019). Magma reservoir failure and the onset of caldera collapse at Kīlauea volcano in 2018. *Science*, *366*(6470).

Delaney, P. T., & Pollard, D. D. (1981). *Deformation of host rocks and flow of magma during growth of minette dikes and breccia-bearing intrusions near ship rock, new mexico* (Vol. 1202; Tech. Rep.). USGS.

Dietterich, H. R., Diefenbach, A. K., Soule, S. A., Zoeller, M. H., Patrick, M. P., Major, J. J., & Lundgren, P. R. (2021). Lava effusion rate evolution and erupted volume during the 2018 Kīlauea lower East Rift Zone eruption. *Bulletin of Volcanology*, *83*(4), 1–18.

Dzurisin, D., & Poland, M. P. (2018). Magma supply to Kīlauea Volcano, Hawai ‘i, from inception to now: Historical perspective, current state of knowledge, and future challenges. *Field volcanology: A tribute to the distinguished career of Don Swanson, Geological Society of America Special Paper*, *538*, 275–295.

Gansecki, C., Lee, R. L., Shea, T., Lundblad, S. P., Hon, K., & Parcheta, C. (2019). The tangled tale of Kīlauea’s 2018 eruption as told by geochemical monitoring. *Science*, *366*(6470).

Gonnermann, H. M., Johanson, I. A., Patrick, M. R., & Anderson, K. R. (2019). Numerical modeling of down-rift pressure surges from episodic caldera collapse during the 2018 Kīlauea eruption. In *Agu fall meeting abstracts* (Vol. 2019, pp. V43C–0214).

Montagna, C. P., & Gonnermann, H. M. (2013). Magma flow between summit and Pu ‘u ‘ō ‘ō at Kīlauea volcano, Hawai ‘i. *Geochemistry, Geophysics, Geosystems*, *14*(7), 2232–2246.

Neal, C., Brantley, S., Antolik, L., Babb, J., Burgess, M., Calles, K., ... others (2019). The 2018 rift eruption and summit collapse of Kīlauea volcano. *Science*, *363*(6425), 367–374.

Nooner, S. L., & Chadwick, W. W. (2016). Inflation-predictable behavior and co-eruption deformation at Axial Seamount. *Science*, *354*(6318), 1399–1403.

Owen, S., Segall, P., Lisowski, M., Miklius, A., Murray, M., Bevis, M., & Foster, J. (2000, Sep). January 30, 1997 eruptive event on Kilauea volcano, Hawaii, as monitored by continuous gps. *Geophys. Res. Letters*, *27*(17), 2757 – 2760.

Patrick, M., Dietterich, H., Lyons, J., Diefenbach, A., Parcheta, C., Anderson, K., ... Kauahikaua, J. (2019). Cyclic lava effusion during the 2018 eruption of Kīlauea volcano. *Science*, *366*(6470).

Segall, P. (2013). Volcano deformation and eruption forecasting. *Geological Society,*

London, Special Publications, *380*.

Segall, P., & Anderson, K. (2021). Repeating caldera collapse events constrain fault friction at the kilometer scale. *Proceedings of the National Academy of Sciences*, *118*(30).

Segall, P., Anderson, K. R., Pulvirenti, F., Wang, T., & Johanson, I. (2020). Caldera collapse geometry revealed by near-field GPS displacements at Kīlauea volcano in 2018. *Geophysical Research Letters*, e2020GL088867.

Sturkell, E., Einarsson, P., Sigmundsson, F., Geirsson, H., Olafsson, H., Pedersen, R., ... Stefánsson, R. (2006). Volcano geodesy and magma dynamics in Iceland. *Journal of Volcanology and Geothermal Research*, *150*(1-3), 14–34.

Tepp, G., Hotovec-Ellis, A., Shiro, B., Johanson, I., Thelen, W., & Haney, M. M. (2020). Seismic and geodetic progression of the 2018 summit caldera collapse of Kīlauea volcano. *Earth and Planetary Science Letters*, *540*, 116250.

Thornber, C. R., Heliker, C., Sherrod, D. R., Kauahikaua, J. P., Miklius, A., Okubo, P. G., ... Meeker, G. P. (2003). Kilauea East Rift Zone magmatism: an episode 54 perspective. *J. Petr.*, *44*, 1525-1559.

Wang, T., Coppess, K., Segall, P., Dunham, E., & Ellsworth, W. (2022). Physics-based model reconciles caldera collapse induced static and dynamic ground motion: application to Kīlauea 2018. *Geophysical Research Letters*.

Wang, T., Zheng, Y., Pulvirenti, F., & Segall, P. (2021). Post-2018 caldera collapse re-inflation uniquely constrains Kīlauea's magmatic system. *Journal of Geophysical Research. Solid Earth*.

Wright, T. L., & Klein, F. W. (2014). *Two hundred years of magma transport and storage at Kīlauea Volcano, Hawai'i, 1790-2008* (No. Professional Paper 1806). U.S. Geological Survey.